# A comparative study of MATRA-LMR/FB with CFD on a fuel assembly in PGSFR

Jin Yoo [*], Won-Pyo Chang, Jae-Ho Jeong, Kwi-Seok Ha, Kwi-Lim Lee, Seung Won Lee, Chiwoong Choi, Sang-Jun Ahn
*Korea Atomic Energy Research Institute*
*P.O.Box 105, Yuseong, Daejeon, 305-600, Korea*
[*] *Corresponding author: yoojin@kaeri.re.kr*

## 1. Introduction

A partial flow blockage accident in a fuel assembly must be a safety concern in the SFR design. When a partial blockage occurs, the sodium coolant flow would be disturbed in the vicinity of the blockage, and the affected flow could lead to a high local coolant temperature. While the coolant would flow normally along the direction of the fuel assembly, a recirculation region downstream from the blockage could emerge above the blockage. The code, therefore, must be capable of representing such complex thermal-hydraulic phenomena reasonably. In this regard, an analysis code, MATRA-LMR-FB, was developed for the purpose of a flow blockage analysis in Korea [1, 2]. MATRA-LMR-FB is a revised version of MATRA-LMR, which was developed based on the frame of the COBRAIV-i code, initially for application to the core sub-channel analysis of the SFR [3]. Some of its models were modified to be eligible for the analysis of the SFR sub-channel blockage with the wire-wrapped pins. The wire-forcing-function used in the MATRA-LMR, which allocates a forced flow with an empirical correlation for the flow effect of the wire-wrap, was replaced with the Distributed Resistance Model [4]. The Distributed Resistance Model has generally been believed to represent the effect more realistically than the wire-forcing-function. A semi-implicit numerical method was applied to resolve a flow reversal problem, which could not be handled by the former fully implicit method. The differencing scheme was also modified to obtain a stable solution with a reduced numerical diffusion. The turbulent mixing model as well as the transient time-step control was improved for efficiency. Because a practical blockage usually makes a permeable medium rather than an impermeable one, a porous blockage model was incorporated into it by employing the correlation suggested by Ergun [5]. The MATRA-LMR-FB was qualified based on the available experimental data [1, 2, 6, 7, 8, 9, 10]. A code-to-code comparison study was also performed as part of an effort to supplement the qualification [11].

Although MATRA-LMR-FB was qualified based on available experimental data including a code-to-code comparative analysis, it was still hard to say that the level of confidence was enough to apply it to the SFR design with full satisfaction. Additional studies are therefore needed to supplement the qualification of MATRA-LMR-FB. In this study, a code-to-code comparative study was conducted as part of an effort to supplement the qualification of MATRA-LMR-FB. The comparison between MATRA-LMR-FB and the CFD code, CFX, was carried out on a 91-pin fuel assembly based on a 217 pin fuel assembly in a PGSFR to assess the MATRA-LMR-FB prediction capability.

## 2. MATRA-LMR/FB Feature

In a sub-channel analysis approach, the flow area of the fuel assembly is divided into a large number of individual flow channels, the sub-channels in Figure 1, whose boundary consists of wall surfaces and gaps between walls. There are three types of sub-channels in MATRA-LMR-FB, namely, internal, edge, and corner sub-channels. Figures 1 and 2 show the representative sub-channels chosen for analysis.

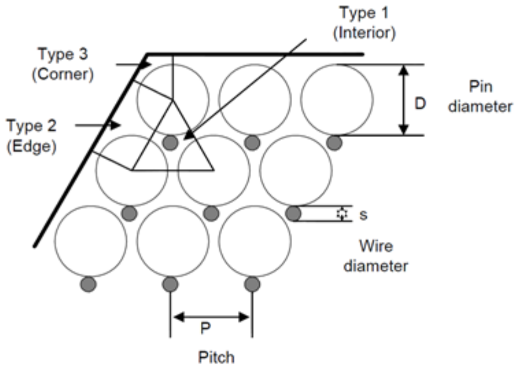


**Figure 1. Sub-channel types of MATRA-LMR/FB**

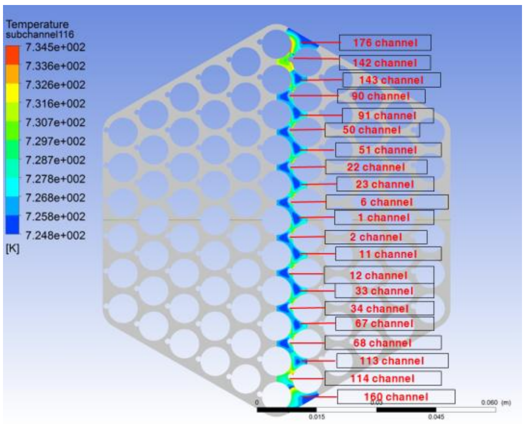


**Figure 2. Predicted sub-channel number**

## 3. Analysis

### *3.1 PGSFR fuel assembly*

Figure 3 shows a lateral view sketch of the PGSFR fuel assembly. The fuel assembly of the PGSFR has 217-pin rods helically wire-wrapped, with rod diameter d = 7.4 mm, pitch-to-diameter ratio p/d = 1.203, and active length L = 900 mm. The total thermal power of the fuel assembly is Q–5.1 MW. However, the fuel assembly having a 91-pin rod shown in Figure 4 was considered to restrict the limitations of the required computer memory in this study. The main design parameters used in the calculation are listed in Table 1.

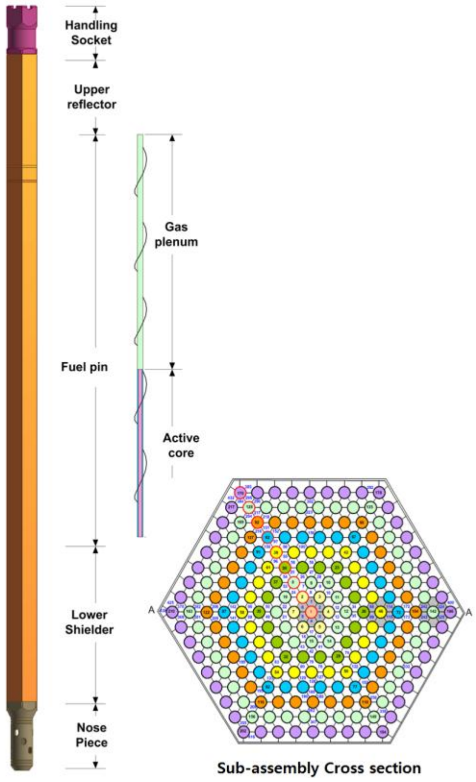


**Figure 3. Fuel assembly with 217-pin rods**

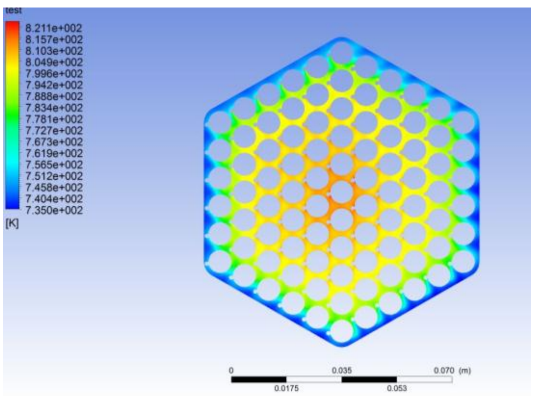


**Figure 4. Fuel assembly with 91-pin rods**

**Table 1. Design parameters of the fuel assembly**

| Parameters | Unit | - |
|---|---|---|
| Number of Pins | EA | 91 |
| Diameter of Pins | mm | 7.4 |
| Pin Pitch | mm | 8.9 |
| Pitch to diameter | - | 1.203 |
| Active core length | mm | 900 |
| Wire wrap Pitch | mm | 183.8 |
| Diameter of Spacer Wire | mm | 1.4 |
| Inner Flat-to-flat Distance | mm | 90.604 |
| Range of Reynold number | - | 50000 |

### *3.2 Computational Boundary Conditions and turbulent model*

The boundary conditions imposed on this study are presented in Figure 3. The inlet conditions were imposed with a mass flow rate of 11.41 kg/s, and a constant temperature of 663.15 K, which are equivalent to the assembly conditions with a 217 fuel pin. In addition, the outlet condition was imposed on the relative pressure of 0 Pa. Figure 5 shows the axial heat flux of the fuel assembly in PGSFR. The heat flux distributions were imposed on the inner cladding surface. And as the outer cladding, the wire was defined with no slip conditions, a conservative interface flux, and a smooth surface. The hexagonal wall of fluid is taken to be adiabatic. The flow blockage was assumed to take place near the axial position with the highest heat flux in Figure 6. The assumption was based on the background that the coolant heat-up would be large at that position, because the flow would slow down or may be temporarily stagnant in the vicinity of the blockage.

For the CFD analysis, it is very important which turbulent model should be used for this analysis. The SST model performs well for cases of adverse pressure gradients and separated flow. This structural feature of the model to predict in a good way the flow separation and recirculation provides good confidence in applying the model to compute the flow blockage in the fuel assembly. Therefore, the SST model was used for a comparison between two codes. The high-resolution scheme was used for the convective term. Convergence of the simulation was judged by the periodic temperature on the outlet domain of the 91-pin fuel assembly.

The scheme zone for analysis using the MATRA-LMR/FB was modeled the same as a CFD. The node size was roughly divided into the length (3.0 cm) along the axial direction and total numbers of the nodes were divided into the same size.

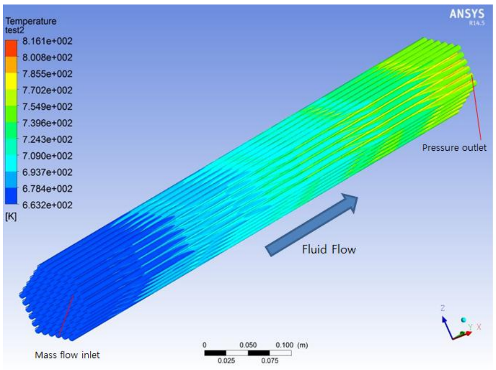


**Figure 5. Boundary conditions**

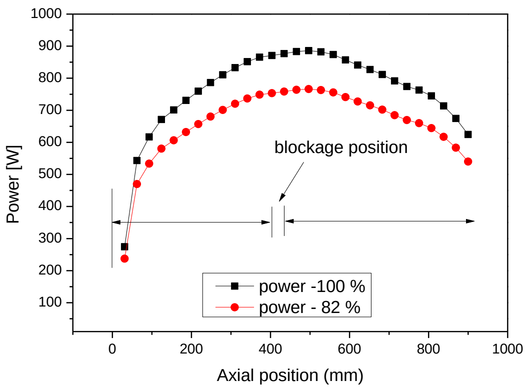


**Figure 6. Fuel assembly with 217-pin rods**

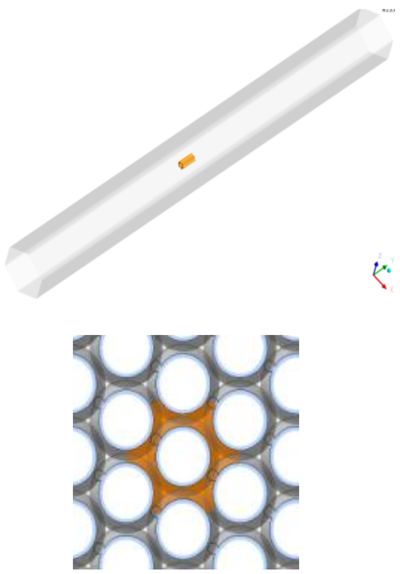

**Figure 7. Blockage position**

## 4. Results

### *4. 1 Without blockage*

The solution without a blockage is analyzed as a reference to check whether the model provides reasonable results and to have the baseline to evaluate the effect of the blockage. Figure 8 shows the temperature distribution in a transversal plane calculated at 440 mm, 470 mm, and 900 mm positions. It shows that the coolant temperature gradually increases as it flows upward along the end of the active region, and the maximum sub-channel temperature is predicted at the end of active core to be about 455℃, 460 ℃, and 530 ℃, respectively. For the internal channel, it shows that the sub-channel temperature predicted by two codes has a similar tendency., i.e., #90, #91, #50, #51, #22, #23, #6, #1, #2, #11, #12, #33, #34, #67, and #68, whereas for a peripheral channel, those have a somewhat difference with a maximum deviation of 25℃, i.e., #176, #142, #143, , #113 #114, and #160. Figure 9 shows the velocity distribution of the fluid at 440 mm and 900 mm positions from the start of the inlet. For the CFD, the velocity distribution is not evenly balanced at a 440 mm position from the inlet. It needs more length to be fully developed. In addition, the velocity in peripheral channels # 176 and #160 calculated by the MATRA-LMR-FB has larger values compared to the CFD.

Figures 10 and 11 show the temperature and velocity distributions of two codes in a transversal plane. Considering the MATRA-LMR-FB results, it was confirmed that the peripheral channel prediction calculated by different pressure drop models, which are Novendstern, Chiu Rohsenow-Todreas, and Cheng-Todreas, were quite different between two codes. From these results, two codes have a similar tendency in a central channel.

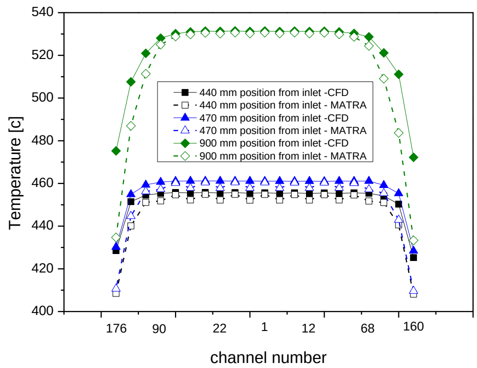


**Figure 8 Temperature distributions in a transversal plane along the streamwire direction**

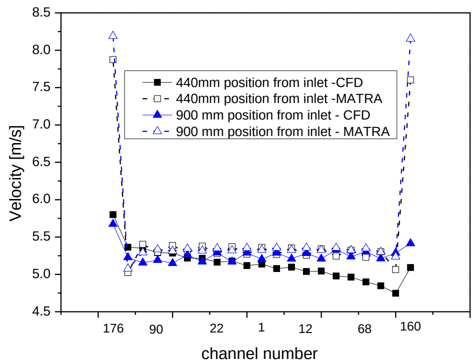


**Figure 9 Velocity distributions in a transversal plane**

**along the streamwire direction**

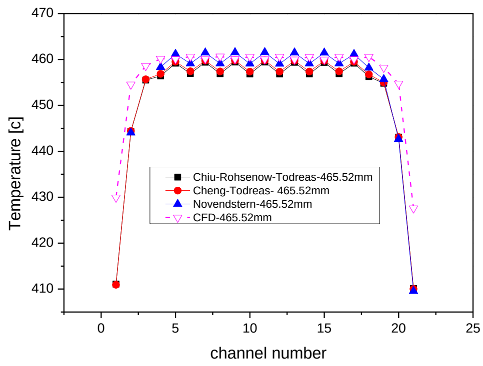


**Figure 10 Temperature distributions of two codes in a transversal plane**

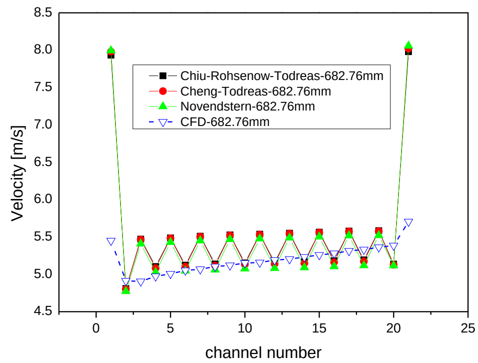


**Figure 11 Velocity distributions of two codes in a transversal plane**

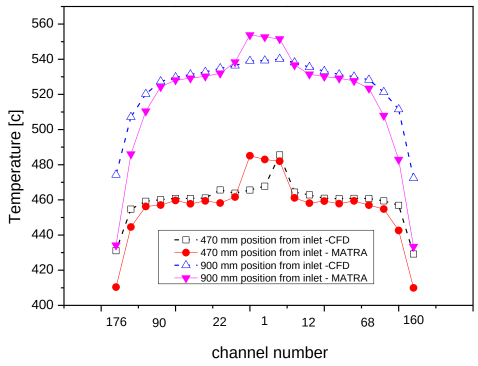


**Figure 12 Temperature distributions in a transversal plane along the streamwire direction**

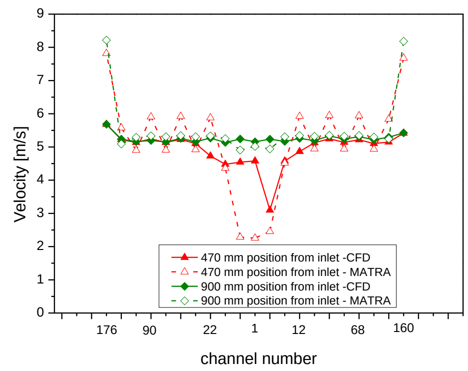


**Figure 13 Velocity distributions along the streamwire direction**

*4. 2 With blockage*

Figure 12 shows the temperature contours in a transversal plane calculated at 470 mm and 900 mm pos itions downstream from the blockage. The temperature distribution calculated by two codes is increased linearly as it flew upward along the end of the active region. In terms of the flow blockage phenomena predicted by two codes, both codes predict that not only the distinct peak temperature but also its maximum temperature downstream from the blockage are 480 ℃. For the CFD analysis results, however, the effect of the blockage seems to be alleviated because the temperature distribution is almost even at the end of active core, whereas for MATRA-LMR-FB, the peak temperature caused by the blockage lasts until the exit of the fuel assembly. Figure 13 shows the velocity distribution calc ulated at 470 mm and 900 mm positions. Although the velocity distribution calculated by the two codes show quite different results in peripheral regions of #176 and #160, it has a similar tendency for the rest of the channels. In particular, abruptly decreased velocities caused by recirculation show similar results for the two codes.

## 5. Conclusions

The prediction of the MATRA-LMR-FB code was co mpared with the CFD using a 91-pin fuel assembly. Mos t sub-channels calculated by MATRA-LMR-FB showed similar results as those calculated by the CFD. The central channel predicted by MATRA-LMR-FB had a g ood agreement with that predicted by the CFD. However, for the edge channel, it showed a large differe nce between the two codes. The temperatures predicted by the MATRA-LMR-FB in an edge channel were under-predicted, whereas the velocity was over-predicte d. In terms of the flow blockage phenomena, two codes showed a similar peak temperature right behind the bloc kage. However, the effect of the blockage predicted by MATRA-LMR-FB seems to last until the exit of the fuel assembly.

More validation using the experimental data for the MATRA-LMR-FB code is required.

## REFERENCES

[1] Ha, K. S., Jeong, H. Y., Chang, W. P., Kwon, Y. M., Cho, C.H., and Lee, Y. B., 2009. Development of the

MATRALMR-FB for Flow Blockage Analysis in a LMR," Nucl. Eng. Tech. 41, 6, 797-806.

[2] Jeong, H. Y., Ha, K. S., Chang , W. P., Kwon, Y. M., and Lee, Y. B., 2005. Modeling of Flow Blockage in a Liquid Metal. Cooled Reactor Subassembly With a Subchannel Analysis Code. Nuclear Technology 149, 71-87.

[3] *Kim, W. S., Kim, Y. K., and Kim, Y. J., 1998. MATRALMR Code Development for LMFBR Core Subchannel Analysis. KAERI/TR-1050/98, Korea Atomic Energy Research Institute.

[4] Ninokata H., et al., 1987. Distributed Resistance Model of Wire-Wrapped Rod Bundles. Nucl. Eng. Des. 104, 93-102.

[5] Ergun, S., 1952. Fluid flow through packed columns. Chem. Eng. Prog. 48 (2), 89-94.

[6] Fontana, M. H. et al., "Temperature distribution in the duct wall and at the exit of a 19-rod simulated LMFBR fuel assembly (FFM Bundle 2A)," Nucl. Technol., 24, 176-200,
(1974).

[7] Domanus, H. M., Shah, V. L. and Sha, W. T., "Applications of the COMMIX code using the porous mediumformulation,"Nucl. Energ. Des., 62, 81-100, (1980).

[8] Haga, K. et al., 1981, Experiments on Local Core Anomaly Detection by Fluctuations of Temperature and Flow Rate at LMFBR Fuel Subassembly Outlets, PNC N 941 81-18, PNC N941 81-74, pp. 5-31 ~ 5-41, PNC, (1981).

[9] Huber, F. and Peppler, W., "Summary and Implications of Out-of-pile Investigations of Local Cooling Distributions in LMFBR Subassembly Geometry under Single-phase and Boiling Conditions," KfK 3927, Kernforschungszentrun Karlsruhe, (1985).

[10] Olive, J. and Jolas, P., "International Blockage in a Fissile Super-Phenix Type Subassembly: The Scarlet Experiments and Their Interpretation by The Cafca-NA3 Code," Nucl. Energy, 4, 287, (1990).

[11] Chang, W.P., Ha, K.S., Suk, S. D., and Jeong, H.Y., 2011. A Comparative study of the MATRA-LMR-FB calculation with the SABRE result for the flow blockage accident in the sodium cooled fast Reactor. Nucl. Eng. Des. 241, 5225-5237.

[12] Kim, W. S., Kim, Y. G. and Kim, Y. J., "A Sub-channel Analysis Code MATRA-LMR for Wire-Wrapped LMR subassembly," Annals of Nuclear Energy, 29, 303, 2002.

[13] Stewart, C. W., Wheeler, C. L., Cena, R. J.,McMonagle, C. Cuta, A. J. M. and Trent, D. S., "COBRA-IV : The model and the method," BNWL-2214, Pacific Northwest Laboratoies, 1977.

[14] Peter Ray Diller. (2005). "Wire Wrapped Fuel Pin Hexagonal Arrays for PWR Service," the degree of master, Massachusetts Institute of Technology.